Changes in patient peripheral blood cell microRNAs after total body irradiation during hematopoietic stem cell transplantation

Juan-Juan Li[1#^], Lei Xu[2#], Cheng-Long Wang[3], Jing-Wen Niu[2], Xuan Zou[3], Xuan-Qi Feng[4], Rong-Jian Lu[3]

[1]Laboratory of Tissue Regeneration and Immunology and Department of Periodontics, Beijing Key Laboratory of Tooth Regeneration and Function Reconstruction, Capital Medical University School of Stomatology, Beijing, China; [2]Department of Hematopoietic Stem Cell Transplantation, Fifth Medical Center, Chinese PLA General Hospital, Beijing, China; [3]Department of Stomatology, Fifth Medical Center, Chinese PLA General Hospital, Beijing, China; [4]Medical School of Chinese PLA, Beijing, China

Contributions: (I) Conception and design: JJ Li; (II) Administrative support: RJ Lu; (III) Provision of study materials or patients: L Xu; (IV) Collection and assembly of data: CL Wang; (V) Data analysis and interpretation: JW Niu, XQ Feng; (VI) Manuscript writing: All authors; (VII) Final approval of manuscript: All authors.

[#]These authors contributed equally to this work.

Correspondence to: Rong-Jian Lu. Department of Stomatology, Fifth Medical Center, Chinese PLA General Hospital, No. 8 of Dongda Street, Fengtai District, Beijing 100071, China. Email: 13426301158@163.com.

Background: Ionizing radiation exposure is a great threat to human health. MicroRNAs (miRNAs) have been shown to play an important role in radiation-induced biological effects. Here, we investigated plasma miRNA expression changes and differentially expressed miRNAs in radiotherapy patients exposed to cobalt-60 (^{60}Co) gamma rays to provide an experimental basis for human plasma miRNAs as an estimation indicator for ionizing radiation injury.

Methods: Six patients with acute lymphoblastic leukemia (ALL) received continuous 5 gray (Gy) total body irradiation (TBI) twice. At 12 hours after irradiation, miRNA microarray was applied to screen for differentially expressed miRNAs, with some miRNAs confirmed by real-time polymerase chain reaction (RT-PCR) assay. Bioinformatic analysis was carried out to identify the relevant target genes and biological function of the differentially expressed miRNAs.

Results: After radiotherapy patients were exposed to 5 Gy gamma radiation, the expression of 9 plasma miRNAs was significantly upregulated, and the expression of 2 miRNAs was downregulated. After irradiation with 10 Gy gamma radiation, the blood plasma of radiotherapy patients contained 18 differentially expressed miRNAs, of which 17 were upregulated and 1 was downregulated ($P<0.05$). The expression of miR-4532, miR-4634, miR-4655-5p, miR-4763-3p, miR-4785, miR-6087, miR-6850-5p, and miR-6869-5p were significantly upregulated in both the 5-Gy and 10-Gy dose groups, showing a certain dose-response relationship. The RT-PCR results were consistent with the findings of high-throughput sequencing. In addition, the target genes of the differentially expressed miRNAs were mainly involved in RNA transcription and DNA damage. Kyoto Encyclopedia of Genes and Genomes (KEGG) enrichment analysis revealed that these miRNAs participated in phosphoinositide 3-kinase/protein kinase B (PI3K/AKT), Ras, mitogen-activated protein kinase (MAPK), and other signaling pathways.

Conclusions: The expression of differential plasma miRNAs of radiotherapy patients was associated with irradiation injury and showed a certain dose-effect relationship. These differentially coexpressed plasma miRNAs could be used as an early indicator for estimating radiation injury.

Keywords: Ionizing radiation; microRNA; total body irradiation (TBI); hematopoietic stem cell transplantation (HSCT)

^ ORCID: 0000-0003-1175-3991.

Submitted May 17, 2022. Accepted for publication Aug 15, 2022.
doi: 10.21037/atm-22-3411
View this article at: https://dx.doi.org/10.21037/atm-22-3411

Introduction

With the wide application of nuclear technology to processes such as radiation sterilization, medical diagnosis, radiotherapy, and nuclear weapons, among others. the potential risk of ionizing radiation exposure in humans is increasing (1,2). Ionizing radiation can directly or indirectly cause severe biological effects by inducing the organism to produce large numbers of free radicals, leading to cell apoptosis, gene mutation, chromosome aberration, DNA damage, and micronucleus formation, which seriously endangers human health and safety (3-5). The prevention and treatment of ionizing radiation injury is currently attracting considerable attention and has become an important research topic in the field of radiation biology.

Rapid and accurate determination of the dose of radiation exposure in individuals is key to successful treatment and is important for improving therapeutic effect and rescue efficiency (6). However, traditional methods for estimating radiation dosage have shortcomings, such as the inclusion of cumbersome steps, the amount of time required, and narrow detection range, rendering them unable to satisfy the demand for large-scale sample detection in a nuclear event (7). Thus, the identification of new biomarkers and detection methods for early-stage ionizing radiation injury has become a focus of research at home and abroad.

As an important molecule in the regulatory network of gene expression, microRNA (miRNA) has high sensitivity and specificity for diagnosis, treatment, and prognostic evaluation of diseases (8-11). Recent studies have shown that the expression level of blood miRNAs is related to radiation dose (12,13). However, current research has been confined to cell- or animal-based experiments, and there are few reports on plasma miRNAs in humans exposed to radiation (14,15).

As it is not possible to obtain healthy people for radiation exposure research, the present study involved acute lymphoblastic leukemia (ALL) patients undergoing whole-body irradiation as subjects. Total body irradiation (TBI) is a commonly used conditioning regimen for hematopoietic stem cell transplantation (HSCT). The success rate of hematopoietic stem cell transplantation can be increased with the use of total body radiation therapy in the pretreatment phase and the recurrence rate drops (16,17). TBI results in multiple organ injury, and it can damage the gastrointestinal (GI), cerebrovascular, hematopoietic, or central nervous systems depending on the total dose of radiation received (18). With the improvements in TBI delivery, dose fractionation, reduction in lung doses and better supportive care measures, the incidence is dropping now. And it is important that patients are closely monitored and counselled on ways to minimize their risk of developing a secondary malignancy, including the role of diet, exercise, alcohol consumption, and abstinence from smoking (19).

Through microarray screening of plasma miRNAs in response to different doses of cobalt-60 (^{60}Co) gamma radiation, validation of real-time quantitative polymerase chain reaction (RT-PCR), and biofunctional analysis, plasma miRNAs with potential as radiation biomarkers were identified to promote the exploration of new methods for radiation injury estimation. We present the following article in accordance with the MDAR reporting checklist (available at https://atm.amegroups.com/article/view/10.21037/atm-22-3411/rc).

Methods

Patient information and plasma preparation

Between June 2018 and August 2019, 6 acute leukemia patients (3 males and 3 females) undergoing total body irradiation (TBI) at the Hematopoietic Stem Cell Transplantation Department of Fifth Medical Center, Chinese PLA General Hospital were recruited for this study (*Table 1*). The study was conducted in accordance with the Declaration of Helsinki (as revised in 2013). All experiments were approved by the research ethics committee of Fifth Medical Center, Chinese PLA General Hospital (No. ky-2018-4-26). All patients voluntarily participated in this study and provided informed consent, and for the patient under age 18 years old, informed consent was also obtained from the legal guardians.

The inclusion criteria were:

(I) ALL patients who had finished chemotherapy 1 month earlier;

Table 1 Patient information

Patient No.	Sex	Age, years	Group A	Group B	Group C
1	Male	17	8:00 Jun 11, 2018	20:00 Jun 11, 2018	20:00 Jun 12, 2018
2	Female	43	8:00 Dec 11, 2018	20:00 Dec 11, 2018	20:00 Dec 12, 2018
3	Male	38	8:00 Dec 17, 2018	20:00 Dec 17, 2018	20:00 Dec 18, 2018
4	Female	38	8:00 Jan 7, 2019	20:00 Jan 7, 2019	20:00 Jan 8, 2019
5	Male	38	8:00 Aug 17, 2019	20:00 Aug 17, 2019	20:00 Aug 18, 2019
6	Female	40	8:00 Aug 28, 2019	20:00 Aug 28, 2019	20:00 Aug 29, 2019

Group A, before irradiation; Group B, 12 hours after irradiation with the first 5 Gy; Group C, 12 hours after irradiation with the second 5 Gy.

(II) Aged 17–50 years old; and
(III) Prepared for hematopoietic stem cell transplantation and pretreatment regimens including TBI.

The exclusion criteria were:

(I) Patients suffering from other systemic malignancy;
(II) Reception of blood transfusion within 2 days of irradiation; and
(III) Other serious cases that would likely hinder this clinical study.

Patients received TBI with 5 gray (Gy) ^{60}Co gamma rays at a dose rate of 5 centigray (cGy)/minute, 2 days in a row. A 4 mL peripheral blood sample from each patient was collected before and after irradiation. Based on cumulative irradiation dose, blood samples were divided into 3 groups: before irradiation (Group A), 12 hours after irradiation with the first 5 Gy (Group B), and 12 hours after irradiation with the second 5 Gy (Group C). The blood samples were centrifuged at 3,000 rpm for 10 minutes at 4 ℃, and the supernatant was transferred to an RNA-free centrifuge tube. The plasma was then separated from the supernatant by centrifugation for 15 minutes at a speed of 10,000 rpm. All plasma samples were stored at −80 ℃ prior to any experimentation.

RNA isolation

Chloroform was added to the plasma samples, which were then centrifuged at 12,000 rpm for 5 minutes. Th supernatant was transferred to a new tube, followed by the addition of isopropanol and then centrifuged at 12,000 rpm for 30 seconds. After the supernatant was removed, the pellet was dissolved in RNase-free water, and miRNA was isolated using mirVana™ PARIS™ Kit (Thermo Fisher Scientific, Waltham, MA, USA) following the manufacturer's protocol. Total RNA was quantified by NanoDrop ND-2000 (Thermo Fisher Scientific) and RNA integrity was assessed using the Agilent Bioanalyzer (Agilent Technologies, Santa Clara, CA, USA). The optical density (OD) 260/280 value of the sample RNA was measured with RNase-free water as the control, and a ratio of 1.8–2.0 was deemed acceptable.

Hybridization, washing, and scanning of miRNA microarrays

Total RNA was dephosphorylated, denatured, and labeled with Cyanine-3-CTP following the procedure of the miRNA Complete Labeling and Hybridization Kit (Agilent Technologies). After purification, the labeled RNAs were hybridized onto the Human miRNA Microarray (Agilent Technologies). After washing, the arrays were scanned with a microarray scanner (Agilent Technologies). Feature Extraction Software (Agilent Technologies) was then used to analyze array images to obtain raw data, and GeneSpring software (Agilent Technologies) was employed to normalize the raw data by quantile algorithm and analyze the differences between groups.

Differential miRNA screening and bioinformatic analysis

The probes that at least 100% of samples in any 1 condition out of 2 conditions had flags in "Detected" were chosen for further analysis. To identify differentially expressed miRNAs, the threshold set for regulated genes was a fold change ≥2.0 and *t*-test P value ≤0.05. Predicted target genes of differentially expressed miRNAs were obtained through the miRDB and miRWalk databases. Gene Ontology (GO) analysis and Kyoto Encyclopedia of Genes and Genomes (KEGG) analysis were applied to determine the biofunctions and regulated pathways of target genes.

Determination of differential miRNA with quantitative PCR

RT-PCR primer kit (RIBOBIO, Guangzhou, China) was used to determine miRNA expression with quantitative PCR. After mature miRNAs were reverse transcribed, the product was diluted 10 times for PCR. The PCR system included: TaqMan MicroRNA Assay 20×1.0 μL, 2 μL reverse-transcription reaction product (minimum 1:10 dilution), TaqMan 2× Universal PCR Master Mix (10 μL), and nuclease-free water (7 μL). After denaturation at 95 ℃ for 15 seconds, annealing was performed at 60 ℃ for 20 seconds, with the cycle repeated 40 times. The results of the dissolution curve were drawn at 70–95 ℃, taking 5S ribosomal RNA (5S rRNA) as the reference gene. The expression differences among different groups were calculated by $2^{-\Delta\Delta CT}$, ΔCt = CtmiRNA-CtU6, ΔΔCt = ΔCtM – ΔCtNM.

Statistical analysis

All data were analyzed using SPSS 22.0 software. Measurement data were expressed as ($\bar{x}$±s), with *t*-test used to make comparisons between 2 groups. Chi-square test was used to compare categorical variables. P<0.05 indicated a statistical difference between the 2 groups.

Results

Patient characteristics

Eligible patients were 17 to 50 years of age, had acute myeloid leukemia (AML) or ALL, and were candidates for allo-hematopoietic cell transplantation with TBI-based myeloablative conditioning. To minimize bias, consecutive patients referred to our program from October 2018 through August 2019 who were deemed to be suitable candidates for TBI-based myeloablative conditioning were approached about participating in this study and screened if they gave written consent.

Patients were in complete remission at the start of radiotherapy and had blood cell counts within normal limits. None of the patients had been treated with radiation before. The total dose delivered to patients was 10 Gy in daily fractions of 5 Gy for 2 days, with a 24-hour interval between the 2 fractions of irradiation. Peripheral blood samples were collected and investigated from 6 patients at 3 stages: before TBI and 12 hours after each fraction of TBI.

Differentially expressed miRNAs screening

To identify miRNA profile changes after irradiation, microarray analysis containing 2,570 probes for mature miRNAs was conducted for all 18 samples. The average detection rate was 18.84%, and the average coefficient of variation was 7.9527%, which was under the minimum requirement of 15%. Principal component analysis revealed that the miRNA expression profiles of samples derived from the same patient were close to each other, while those from different patients were relatively discrete. This result suggested that peripheral blood cells from different patients had heterogeneity, and their miRNA profiles after irradiation were quite different.

Twelve differentially expressed plasma miRNAs were detected at 12 hours after irradiation with 5 Gy gamma rays compared with samples before irradiation (*Figure 1*, *Table 2*). Compared with miRNA expression level before irradiation, there were 18 differentially expressed miRNAs at 12 hours after irradiation with 10 Gy, including 17 that were upregulated and 1 that was downregulated (*Figure 1*, *Table 3*). The difference in expression of these plasma miRNAs was statistically significant compared with pre-irradiation (P<0.05). Among them, there were 8 differentially expressed plasma miRNAs in both dosage groups, and all expression levels rose with the accumulation of exposure dosage.

The scatter and volcano plots show the fold change, variation, and distribution of the differentially expressed miRNAs (*Figure 2*). There were 8 differentially coexpressed plasma miRNAs in the 2 dose groups: miR-4532, miR-4634, miR-4655-5p, miR-4763-3p, miR-4785, miR-6087, miR-6850-5p, and miR-6869-5p.

Target genes of differentially expressed miRNAs

The potential target genes of the 7 miRNAs shown in *Table 4* were predicted by the miRWalk and miRDB public databases (*Figure 3*). The top 10 predicted target genes of each miRNA are listed in *Table 4*. These differentially coexpressed miRNAs are mainly involved in the regulation of signal transduction, cell apoptosis, and inflammatory and immune response.

GO analysis showed that the function of the differentially expressed miRNAs on these target genes included protein binding, RNA polymerase II regulatory sequence-specific DNA binding, Rab protein transduction, and regulation of T-cell differentiation, among others (*Figure 4*). KEGG

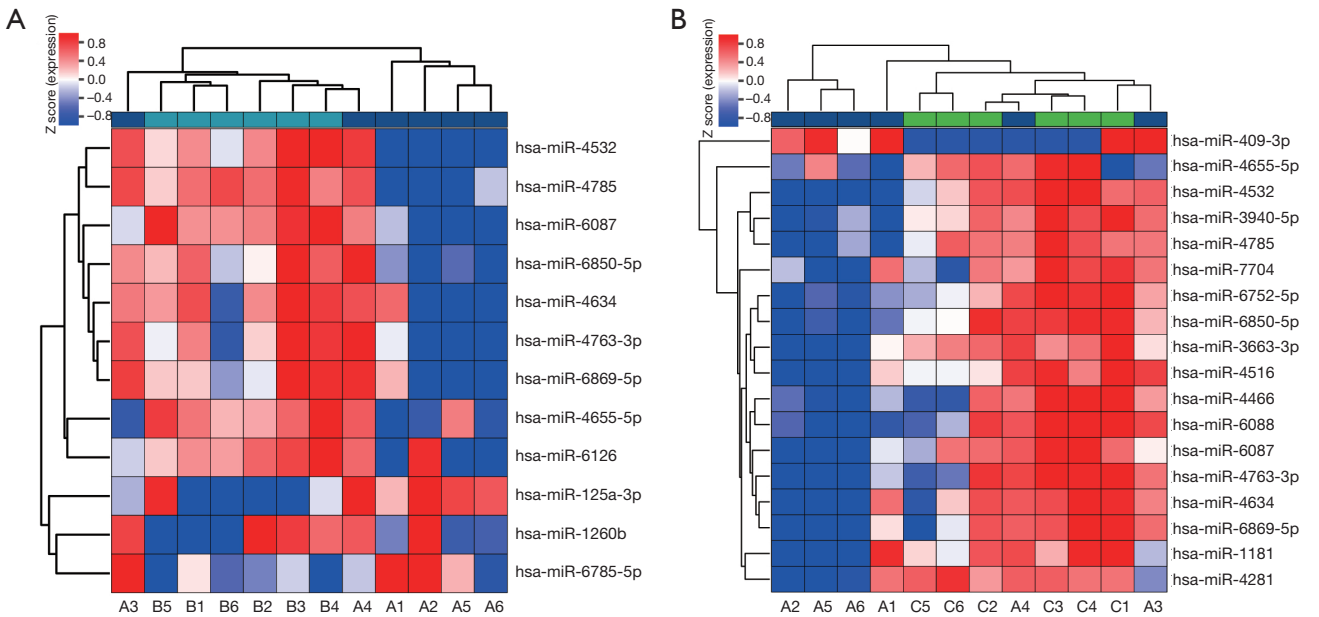

Figure 1 Clustering map of differentially expressed miRNAs between pre-irradiation and different dose irradiation. (A) Clustering map of miRNAs between pre-irradiation and exposure to 5 Gy ^{60}Co. (B) Clustering map of miRNAs between pre-irradiation and exposure to 10 Gy ^{60}Co. The clustering map displays sample name on the X-axes and microRNAs on Y-axes; high expression of miRNAs is presented in red and low is presented in green.

Table 2 Differentially expressed plasma miRNAs after exposure to 5 Gy ^{60}Co

MiRNAs	Sequence	Fold change	Regulated	P value
miR-125a-3p	acaggugagguucuugggagcc	−5.0506	Down	0.0202
miR-1260b	aucccaccacugccaccau	−2.5266	Down	0.0407
miR-4532	ccccggggagcccggcg	8.9484	Up	0.0040
miR-4634	cggcgcgaccggcccgggg	6.1508	Up	0.0443
miR-4655-5p	caccggggauggcagagggucg	2.9456	Up	0.0233
miR-4763-3p	cgccugcccagcccuccugcu	1.6114	Up	0.0255
miR-4785	agagucggcgacgccgccagc	4.9985	Up	0.0385
miR-6087	ugaggcgggggggcgagc	3.1869	Up	0.0064
miR-6126	gugaaggcccggcggaga	6.1444	Up	0.0314
miR-6785-5p	ugggagggcguggaugauggug	−1.9420	Down	0.0153
miR-6850-5p	gugcggaacgcuggccggggcg	1.8832	Up	0.0372
miR-6869-5p	gugaguaguggcgcgcggcggc	1.5485	Up	0.0407

miRNAs, microRNAs; ^{60}Co, cobalt-60.

Table 3 Differentially expressed plasma miRNAs after exposure to 10 Gy ^{60}Co

MiRNAs	Sequence	Fold change	Regulated	P value
miR-409-3p	gaauguugcucggugaaccccu	–5.9508	Down	0.0196
miR-1181	ccgucgccgccacccgagccg	4.5528	Up	0.0324
miR-4281	gggucccggggaggggggg	2.5011	Up	0.0468
miR-3663-3p	ugagcaccacacaggccgggcgc	3.0284	Up	0.0326
miR-4466	gggugcgggccggcgggg	1.5505	Up	0.0034
miR-4516	gggagaagggucggggc	2.4185	Up	0.0413
miR-4532	ccccggggagcccggcg	11.7802	Up	0.0043
miR-3940-5p	gugggguuggggcgggcucug	3.6202	Up	0.0491
miR-4634	cggcgcgaccggcccgggg	6.5470	Up	0.0446
miR-4655-5p	caccggggauggcagagggucg	3.7706	Up	0.0460
miR-4763-3p	aggcaggggcuggugcugggcggg	1.9162	Up	0.0376
miR-4785	agagucggcgacgccgccagc	7.7024	Up	0.0071
miR-6087	ugaggcgggggggcgagc	4.1883	Up	0.0055
miR-6088	agagaugaagcgggggggcg	1.6867	Up	0.0179
miR-6752-5p	gggggguguggagccagggggc	1.6162	Up	0.0346
miR-6850-5p	gugcggaacgcuggccggggcg	2.3780	Up	0.0366
miR-6869-5p	gugaguaguggcgcgcggcggc	1.8093	Up	0.0293
miR-7704	cggggucggcggcgacgug	1.6180	Up	0.0116

miRNAs, microRNAs; ^{60}Co, cobalt-60.

analysis (*Figure 5*, *Table 5*) found that the phosphoinositide 3-kinase/protein kinase B (PI3K/AKT), Ras, and mRNA surveillance signal pathways were activated by target genes in the high-dose group. These pathways were regulated by miR-6850-5p or miR-6869-5p. In the low-dose group, the mitogen-activated protein kinase (MAPK), Ras, and phospholipase D signaling pathways were activated by miR-6869-5p, miR-4655-5p, and miR-4763-3p.

Differential expression validation of miR-4532 and miR-6087

To confirm the differential expression of miR-4532 and miR-6087 pre- and post-irradiation, real-time PCR was performed with 5S rRNA as the reference. The amplification curve displayed a single band and was consistent with the design length, and the melting curve exhibited a single peak, indicating a normal amplification result (*Figure 6*). After ionizing radiation, the expression of miR-4532 and miR-6087 obviously increased with statistical significance, regardless of the irradiation dosage (*Figure 7*). Moreover, the expression level of miR-4532 and miR-6087 in the high-dose group was higher than that in the low-dose group, which was consistent with the microarray determination results.

Discussion

In the case of a large-scale nuclear event, rapid and accurate estimation of exposure dose is essential for the optimal use of medical resources and remedy efficiency (20). Radiobiological effect is the terminal reaction of radiation on the human body, which is in proportion to the exposure dose but free from environmental impact (21). One generally accepted method for estimating the radiation dose of exposed individuals involves taking advantage of biological effect indicators.

Chromosome aberration analysis is most commonly used and regarded as the "gold standard" for estimating radiation dose (22). It is highly reliable and sensitive, but it requires specialized laboratories and is unsuitable for

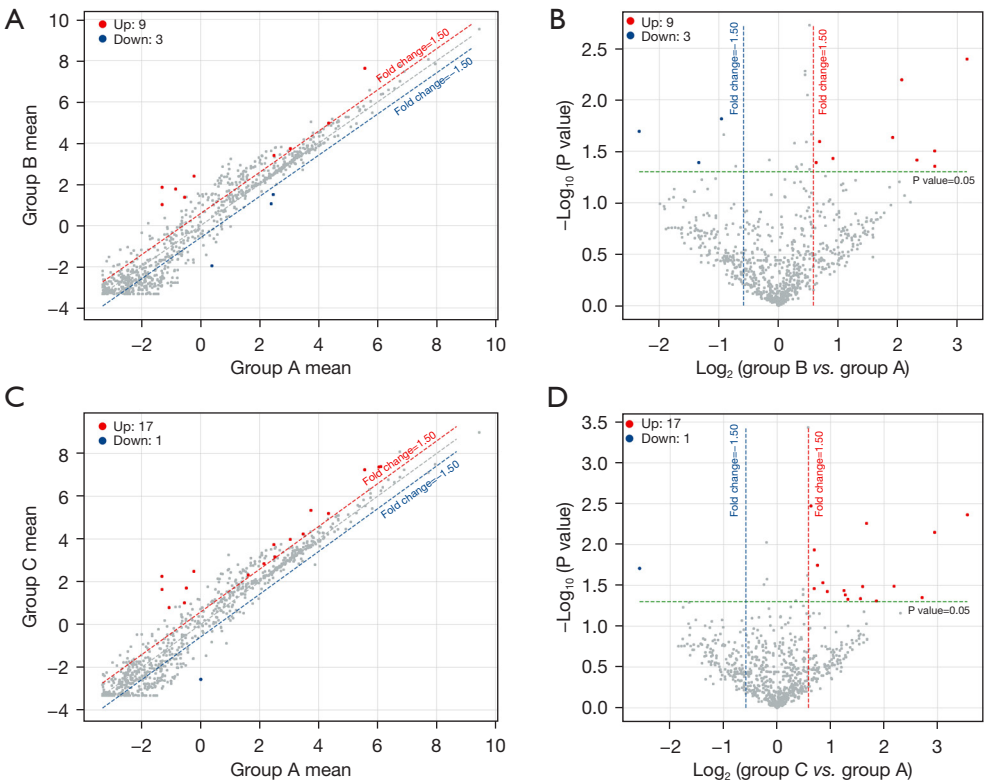

Figure 2 Scatter and volcano plots of differentially expressed miRNAs between pre-irradiation and different dose irradiation. (A) Scatter plot of miRNAs between pre-irradiation and exposure to 5 Gy ^{60}Co. (B) Volcano plot of miRNAs between pre-irradiation and exposure to 5 Gy ^{60}Co. (C) Scatter plot of miRNAs between pre-irradiation and exposure to 10 Gy ^{60}Co. (D) Volcano plot of miRNAs between pre-irradiation and exposure to 10 Gy ^{60}Co. Group A, before irradiation; Group B, 12 hours after irradiation with the first 5 Gy; Group C, 12 hours after irradiation with the second 5 Gy. Grey dots, no differentially expressed miRNAs. miRNAs, MicroRNAs; ^{60}Co, cobalt-60.

Table 4 Partial target genes of coexpressed differentially expressed miRNAs

miRNAs	Partial target genes
miR-4532	*RUNX1, CDC25A, CDKL2, E2F3, MAPK10, HIF3A, CDC25A, AKT1S1, RAD52, MAPKAP1*
miR-4634	*ATM, CDKN2A, GSKIP, AKT1, VEGFA, TGFBR3, ATF5, TNFSF13, EIF2AK2, COLCA2*
miR-4655-5p	*TP53, TNF, IGF2, GTPBP10, PPARD, VEGFB, IER5, FDXR, BRCA1, MAPKBP1*
miR-4785	*SMAD2, MEF2C, MAPK14, RAD18, TNFSF15, E2F2, EIF4G3, HLA-G, GAPDH, ATXN1*
miR-6087	*CDKN2C, FOXF1, WNT9A, MYCT1, RPAP3, TOP3A, SEC62, CDKL3, MMP2, BBC3*
miR-6850-5p	*RUNX1, COL1A1, TNF, NFKB, SMAD2, MAPK10, RAF1, AP2B1, OGDH, CSF1*
miR-6869-5p	*MAPK8, IGF1, BCL2L15, MMP2, EIF4E, PARP9, SAMD9, SEMA4A, MMP2, RAD17*

miRNAs, microRNAs.

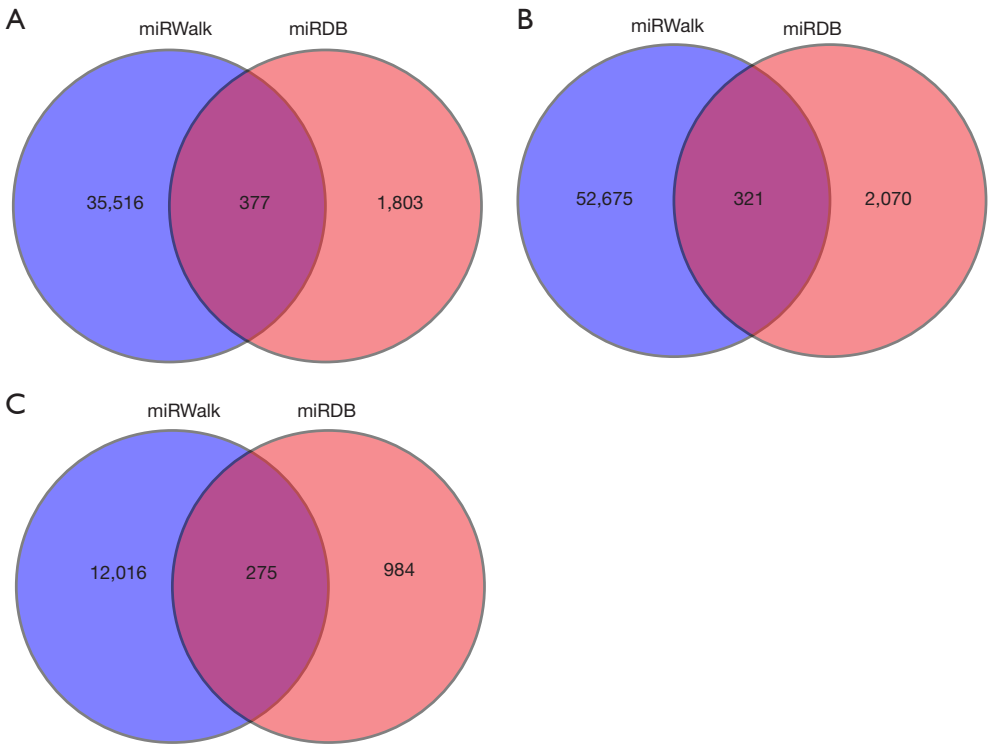

Figure 3 The intersection of target genes in miRDB and miRWalk databases after different dose irradiation. (A) Pre-irradiation versus after irradiation with 5 Gy. (B) Pre-irradiation versus after irradiation with 10 Gy. (C) After irradiation with 5 versus 10 Gy.

batch detection in an accident scene. Its longer reaction time of at least 48–72 hours fails to satisfy the demands of rapid detection (23). Although lymphocyte micronucleus analysis is simple to operate and requires minimal personnel skill, the rapid decline of the lymphocytes greatly affect the accuracy of detection results (24). In addition, single-cell gel electrophoresis analysis based on DNA damage and DNA repair-related protein dosimeters also have some disadvantages, including low sensitivity and numerous interfering factors (25,26). Therefore, it is of great scientific value and practical significance to identify rapid, sensitive, and accurate radiobiological indicators and estimation methods.

MicroRNA is a type of endogenous noncoding small molecule RNA in eukaryotes that plays an important role in biological development, cell apoptosis, gene regulation, and tumor development (27). Ionizing radiation has been shown to induce miRNA expression change, and miRNAs may be a key regulator in radiation stress response. Anastasov *et al.* (28) found the expression of miRNA-21 in breast cancer cells was upregulated at 8 hours post-irradiation with 5 Gy, but after 24 hours, the expression level was equal to that at pre-irradiation. A number of studies have also shown that ionizing radiation could cause miRNA expression changes in skin, lung, and spleen tissues (29-31).

Peripheral blood has stable physical properties and is convenient for collection and rapid detection. The detection of specific markers in peripheral blood has become a research focus in disease diagnosis and prognostic evaluation (32). In recent years, study results have indicated that the expression level of miRNAs in blood is associated with radiation dose (33). Acharya *et al.* found that circulating miR-187-3p, miR-150, and miR-342-3 expression in mice exposed to gamma rays had a close relationship to the radiation dose (12). Wei *et al.* discovered radiosensitivity changes with different radiation doses in circulating miRNAs of mice (34). It has been reported that the expression of blood miRNAs in mice exhibited a dose and time-dependent relationship with X-ray radiation (35). Fendler *et al.* also confirmed the reliability of plasma miRNA of primates as indicators of the biological effects of ionizing radiation (36).

In accordance with medical research ethics, previous studies have focused on cell- or animal-based irradiation experiments, and the results have certain limitations. In this

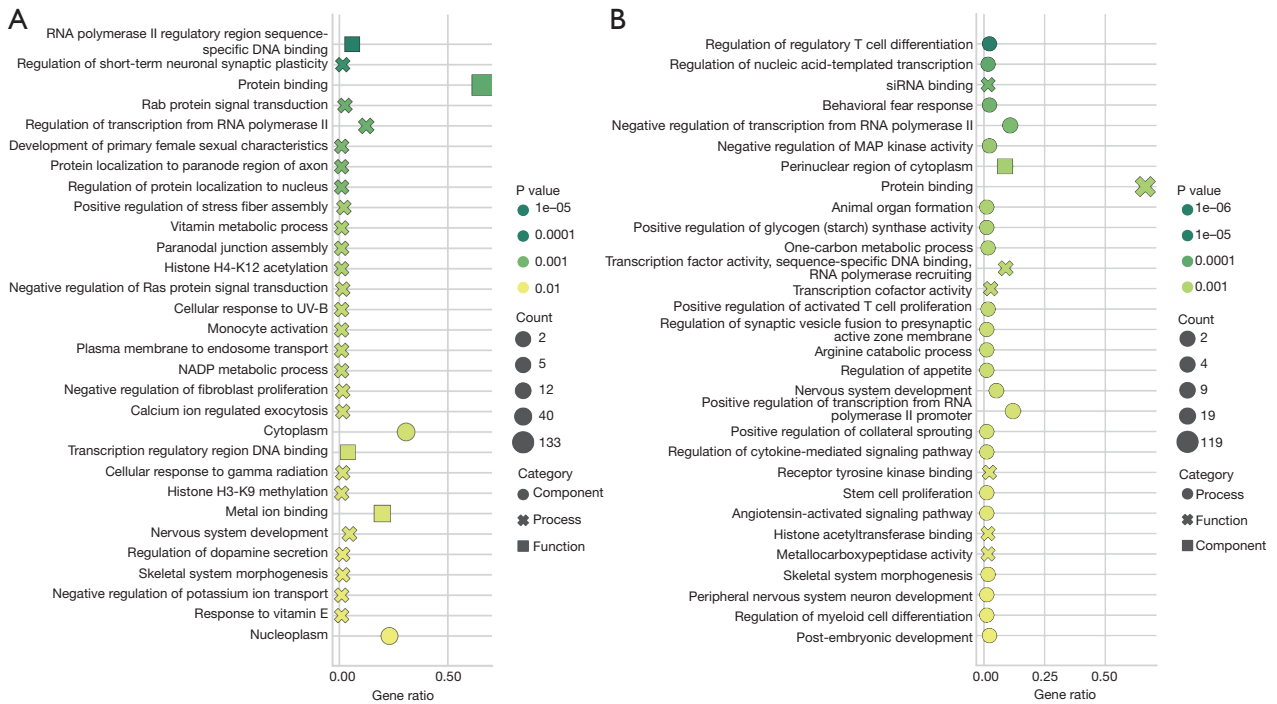

Figure 4 GO analysis on target genes of differentially expressed miRNAs. (A) GO enrichment analysis of target genes between pre-irradiation and exposure to 5 Gy ^{60}Co. (B) GO enrichment analysis of target genes between pre-irradiation and exposure to 10 Gy ^{60}Co. This figure displays the process, function, and component of target genes on Y-axes and degree of enrichment on X-axes. The larger the dot, the more genes involved in the process, function, and component. The greener the color, the higher the significance of enrichment. NADP, nicotinamide adenine dinucleotide phosphate; MAP, mitogen-activated protein; GO, Gene Ontology; miRNAs, microRNAs; ^{60}Co, cobalt-60.

study, subjects were leukemia patients pretreated with total body radiotherapy, which could better simulate the actual radiation condition and ensure radiation effects were free from the influence of different exposure sites and exposure areas. Further, patients did not receive radiotherapy until they had been in remission for 1 month after chemotherapy, and with a small tumor load, the detection results were less susceptible to the effects of other malignancies. For these reasons, these results are more likely to be applied and popularized.

Our results found that several plasma miRNAs of leukemia patients were differentially expressed after exposure to ^{60}Co radiation with different doses, and the difference was statistically significant ($P<0.05$). Remarkably, there were 8 plasma miRNAs exhibiting differential expression in both dose groups (miR-4532, miR-4634, miR-4655-5p, miR-4763-3p, miR-4785, miR-6087, miR-6850-5p, and miR-6869-5p) that all showed upregulation compared to pre-irradiation levels. More importantly, the expression level obviously increased as cumulative exposure doses rose from 5 Gy to 10 Gy. However, unlike previous findings (37), the difference in candidate miRNAs between dose groups was not statistically significant, which may have been due to the smaller sample size and large individual differences of patients.

To date, there are few reports on the ionizing radiosensitivity of differentially coexpressed miRNAs. One recent study (38) showed that miR-4532 could regulate immune reactivity and oxidative stress injury of epithelial cells induced by ultraviolet radiation by stimulating free radical generation to cause cell damage, which is similar to the mechanism of ionizing radiation. MiR-4532 has also been reported to affect the biofunction of hematopoietic stem cells through the signal transducer and activator of transcription 3 (STAT3) signaling pathway, which is closely associated with tumor radiation sensitivity (39,40). Guo *et al.* have reported that miR-125a controls hematopoietic stem cell number by regulating hematopoietic stem/progenitor

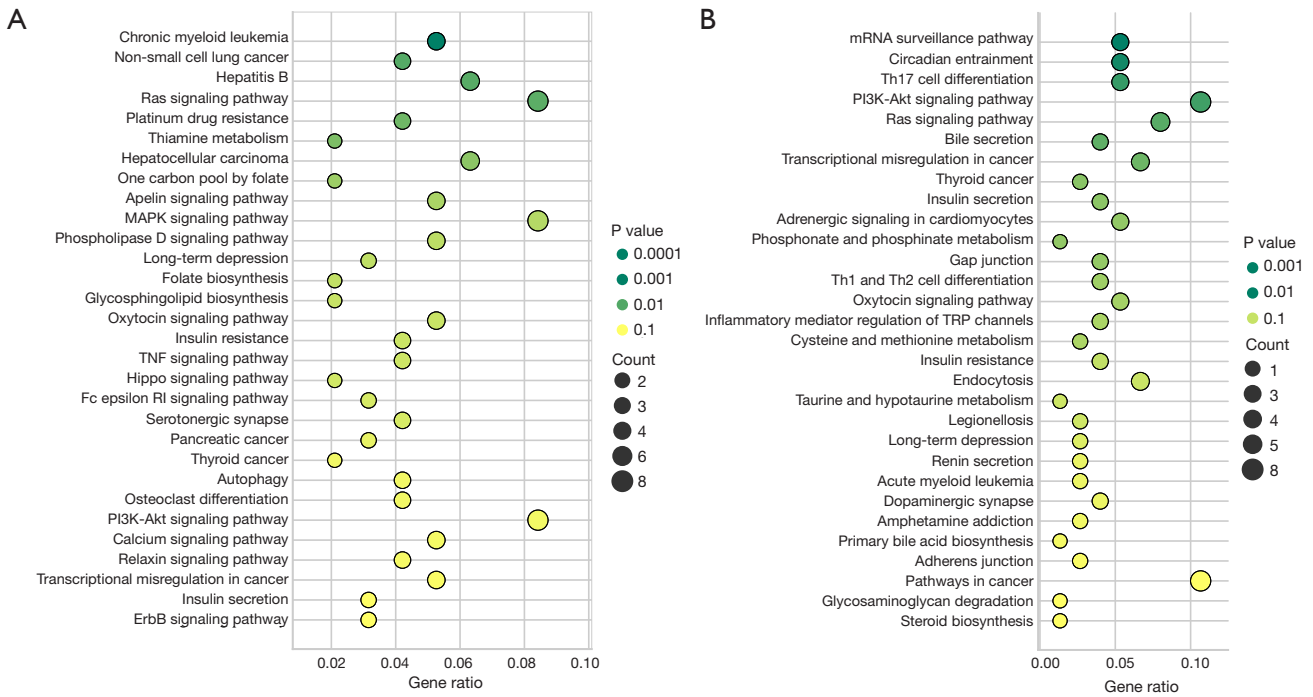

Figure 5 KEGG analysis on target genes of differentially expressed miRNAs. (A) KEGG enrichment of target genes between pre-irradiation and exposure to 5 Gy ^{60}Co. (B) KEGG enrichment of target genes between pre-irradiation and exposure to 10 Gy ^{60}Co. This figure displays signaling pathways on Y-axes and degree of enrichment on X-axes. The larger the dot, the more genes involved in this pathway. The greener the color, the higher the significance of enrichment. KEGG, Kyoto Encyclopedia of Genes and Genomes; miRNAs, microRNAs; ^{60}Co, cobalt-60.

Table 5 Partial KEGG pathways of differentially expressed miRNA regulatory target genes

Pathway ID	Pathway name	Corrected P value	Target gene number	Target gene
hsa04151	PI3K-Akt signaling pathway	0.0265	351	*PPP2R5E; IL2RA; CREB1; IGF2; EFNA5; PHLPP2; RXRA; EIF4E*
hsa04010	MAPK signaling pathway	0.0366	294	*PLA2G4E; RPS6KA2; TGFBR1; ELK1; DUSP4; PRKCA; CSF1; TAOK1*
hsa04014	Ras signaling pathway	0.0113	236	*PLA2G4E; RASSF5; ELK1; GAB2; PRKCA; BCL2L1; CSF1; RAB5B*
hsa04072	Phospholipase D signaling pathway	0.0409	146	*PLA2G4E; AGPAT1; GAB2; PRKCA; GRM4*
hsa03015	mRNA surveillance pathway	0.0139	91	*PPP2R5E; MSI2; HBS1L; SMG7*

KEGG, Kyoto Encyclopedia of Genes and Genomes; miRNAs, microRNAs.

cell (HSPC) apoptosis, which suggests that microRNA-based cell modification may be a means to achieve stem cell-specific therapeutics (41). MiR-6087 has been shown to play an important role in the p53-mediated competing endogenous RNA (ceRNA) network (42). P53 plays a key role in cell DNA damage stress response, and its related genes or proteins are strongly correlated with radiation (43). Another previous study suggested that the expression of miR-4655 was significantly upregulated in apoptosis and oxidative stress induced by nonionizing radiation (44). In our study, we found

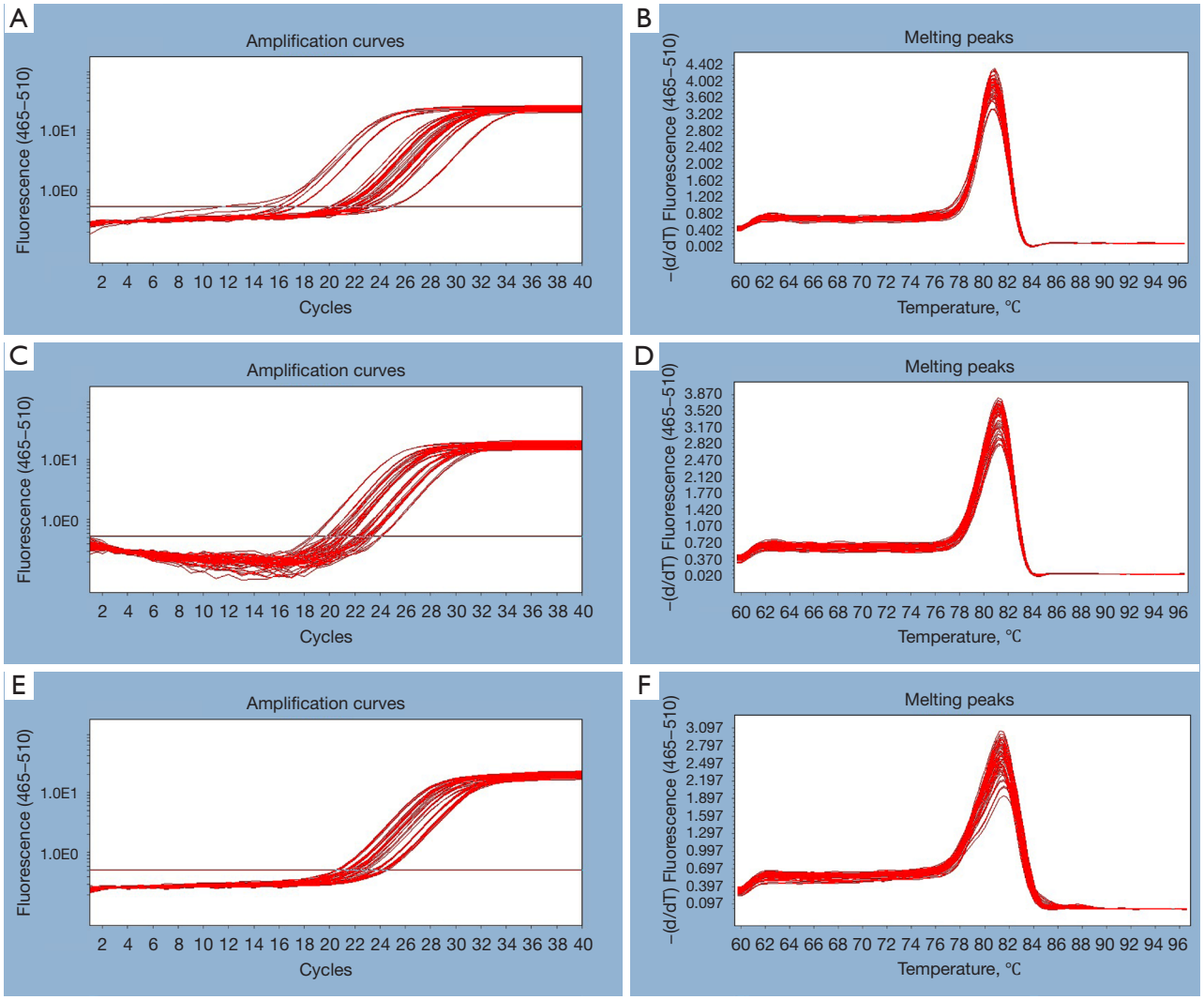

Figure 6 Amplification curve and melting curve for miR-4532, miR-6087, and 5S rRNA. (A) Amplification curve for 5S rRNA; (B) melting curve for 5S rRNA; (C) amplification curve for miR-4532; (D) melting curve for miR-4532; (E) amplification curve for miR-6087; (F) melting curve for miR-6087.

that the expression of miR-4532 was significantly upregulated in both the 5-Gy and 10-Gy dose groups, showing a certain dose-response relationship. We also found miR-125a was significantly downregulated in the 5-Gy dose group. In addition, real-time PCR confirmed the expression level of candidate miRNAs in patients were significantly higher than before radiation. Taken together, it can be concluded that differentially coexpressed plasma miRNAs may have played a certain role in the damaging effect of ionizing radiation.

A wide range of target genes are related to miRNAs involved in regulating ionizing radiation injury. To determine the biological functions of the differentially expressed miRNAs, we performed GO function and KEGG pathway enrichment analysis of the target genes. Bioinformatics analysis revealed that candidate miRNAs mainly regulated the biological processes of transcription, apoptosis, DNA damage, and activation of MAPK, and they largely activated signaling pathways, including PI3K/AKT, MAPK, and Ras, among others, which are involved in radiation oxidative stress and repair of DNA damage. With further research, the function and mechanism of these radiosensitive miRNAs will gradually be clearer.

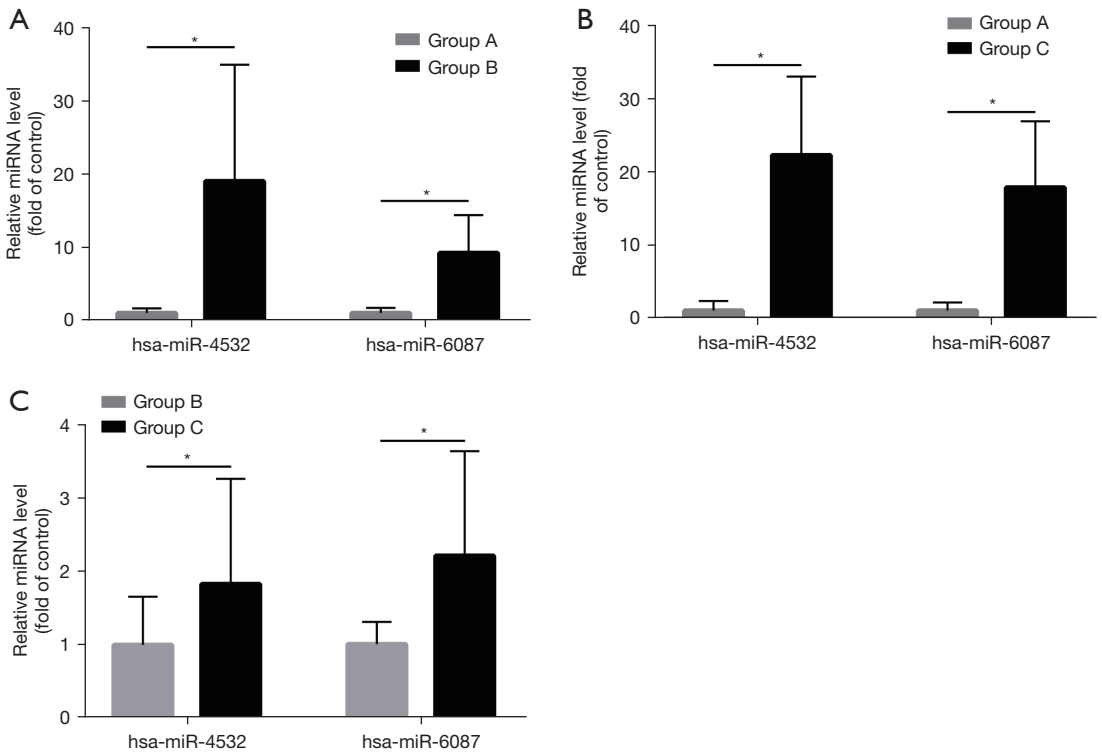

Figure 7 RT-PCR validation of differentially expressed miRNAs. (A) The relative expression of miRNAs between pre-irradiation and the low-dose group. (B) The relative expression of miRNAs between pre-irradiation and the high-dose group. (C) The relative expression of miRNAs in different dose groups. Group A, before irradiation; Group B, 12 hours after irradiation with the first 5 Gy; Group C, 12 hours after irradiation with the second 5 Gy. *, P≤0.05 (unpaired Student's *t*-test). RT-PCR, real-time polymerase chain reaction; miRNAs, microRNAs.

Conclusions

In summary, using microarrays, this study found numerous radiosensitive plasma miRNAs that were associated with immune system and stress responses induced by ionizing radiation. Eight differentially coexpressed plasma miRNAs showed certain dose-dependent changes, and they have the potential to be early biomarkers for estimating radiation. However, the biological function of the candidate miRNAs still needs to be further investigated with large-sample studies.

Acknowledgments

Funding: This study was financially supported by the Military Medical Science and Technology Youth Training Program (No. 18QNP038), Academy of Military Medical Sciences innovation fund (No. 2017CXJJ14), and the Open Project Program of the State Key Laboratory of Proteomics (No. SKLP-O202006).

Footnote

Reporting Checklist: The authors have completed the MDAR reporting checklist. Available at https://atm.amegroups.com/article/view/10.21037/atm-22-3411/rc

Data Sharing Statement: Available at https://atm.amegroups.com/article/view/10.21037/atm-22-3411/dss

Conflicts of Interest: All authors have completed the ICMJE uniform disclosure form (available at https://atm.amegroups.com/article/view/10.21037/atm-22-3411/coif). All authors report that this study was financially supported by the Military Medical Science and Technology Youth Training Program (No. 18QNP038), Academy of Military

Medical Sciences innovation fund (No. 2017CXJJ14) and the Open Project Program of the State Key Laboratory of Proteomics (No. SKLP-O202006). The authors have no other conflicts of interest to declare.

Ethical Statement: The authors are accountable for all aspects of the work in ensuring that questions related to the accuracy or integrity of any part of the work are appropriately investigated and resolved. The study was conducted in accordance with the Declaration of Helsinki (as revised in 2013). All experiments were approved by the research ethics committee of Fifth Medical Center, Chinese PLA General Hospital (No. ky-2018-4-26). All patients voluntarily participated in this study and provided informed consent, and for the patient under age 18 years old, informed consent was also obtained from the legal guardians.

References

1. Wang S, Wang J, Lin S, et al. Public perceptions and acceptance of nuclear energy in China: The role of public knowledge, perceived benefit, perceived risk and public engagement. Energy Policy 2019;126:352-60.
2. Mavragani IV, Nikitaki Z, Souli MP, et al. Complex DNA Damage: A Route to Radiation-Induced Genomic Instability and Carcinogenesis. Cancers (Basel) 2017;9:91.
3. Gudkov SV, Guryev EL, Gapeyev AB, et al. Unmodified hydrated C60 fullerene molecules exhibit antioxidant properties, prevent damage to DNA and proteins induced by reactive oxygen species and protect mice against injuries caused by radiation-induced oxidative stress. Nanomedicine 2019;15:37-46.
4. Zhou H, Sun F, Ou M, et al. Prior nasal delivery of antagomiR-122 prevents radiation-induced brain injury. Mol Ther 2021;29:3465-83.
5. Li Y, Shen Z, Jiang X, et al. Mouse mesenchymal stem cell-derived exosomal miR-466f-3p reverses EMT process through inhibiting AKT/GSK3beta pathway via c-MET in radiation-induced lung injury. J Exp Clin Cancer Res 2022;41:128.
6. Singh VK, Romaine PL, Seed TM. Medical Countermeasures for Radiation Exposure and Related Injuries: Characterization of Medicines, FDA-Approval Status and Inclusion into the Strategic National Stockpile. Health Phys 2015;108:607-30.
7. Singh VK, Newman VL, Romaine PL, et al. Use of biomarkers for assessing radiation injury and efficacy of countermeasures. Expert Rev Mol Diagn 2016;16:65-81.
8. Anfossi S, Babayan A, Pantel K, et al. Clinical utility of circulating non-coding RNAs - an update. Nat Rev Clin Oncol 2018;15:541-63.
9. Pan G, Liu Y, Shang L, et al. EMT-associated microRNAs and their roles in cancer stemness and drug resistance. Cancer Commun (Lond) 2021;41:199-217.
10. Liu Y, Nie H, Ding Y, et al. MiRNA, a New Treatment Strategy for Pulmonary Fibrosis. Curr Drug Targets 2021;22:793-802.
11. Wang X, He Y, Mackowiak B, et al. MicroRNAs as regulators, biomarkers and therapeutic targets in liver diseases. Gut 2021;70:784-95.
12. Acharya SS, Fendler W, Watson J, et al. Serum microRNAs are early indicators of survival after radiation-induced hematopoietic injury. Sci Transl Med 2015;7:287ra69.
13. Cui M, Xiao H, Li Y, et al. Total abdominal irradiation exposure impairs cognitive function involving miR-34a-5p/BDNF axis. Biochim Biophys Acta Mol Basis Dis 2017;1863:2333-41.
14. Aryankalayil MJ, Martello S, Bylicky MA, et al. Analysis of lncRNA-miRNA-mRNA expression pattern in heart tissue after total body radiation in a mouse model. J Transl Med 2021;19:336.
15. Wang S, Li J, He Y, et al. Protective effect of melatonin entrapped PLGA nanoparticles on radiation-induced lung injury through the miR-21/TGF-β1/Smad3 pathway. Int J Pharm 2021;602:120584.
16. Hill-Kayser CE, Plastaras JP, Tochner Z, et al. TBI during BM and SCT: review of the past, discussion of the present and consideration of future directions. Bone Marrow Transplant 2011;46:475-84.
17. Valente M, Denis J, Grenier N, et al. Revisiting Biomarkers of Total-Body and Partial-Body Exposure in a Baboon Model of Irradiation. PLoS One 2015;10:e0132194.
18. Wambi CO, Sanzari JK, Sayers CM, et al. Protective

effects of dietary antioxidants on proton total-body irradiation-mediated hematopoietic cell and animal survival. Radiat Res 2009;172:175-86.
19. Sabloff M, Tisseverasinghe S, Babadagli ME, et al. Total Body Irradiation for Hematopoietic Stem Cell Transplantation: What Can We Agree on? Curr Oncol 2021;28:903-17.
20. Port M, Hérodin F, Valente M, et al. Persistent mRNA and miRNA expression changes in irradiated baboons. Sci Rep 2018;8:15353.
21. Steinhauser G, Brandl A, Johnson TE. Comparison of the Chernobyl and Fukushima nuclear accidents: a review of the environmental impacts. Sci Total Environ 2014;470-471:800-17.
22. Forster JC, Douglass MJJ, Phillips WM, et al. Stochastic multicellular modeling of x-ray irradiation, DNA damage induction, DNA free-end misrejoining and cell death. Sci Rep 2019;9:18888.
23. Kato TA. Human Lymphocyte Metaphase Chromosome Preparation for Radiation-Induced Chromosome Aberration Analysis. Methods Mol Biol 2019;1984:1-6.
24. Nautiyal A, Mondal T, Mukherjee A, et al. Quantification of DNA damage in patients undergoing non-contrast and contrast enhanced whole body PET/CT investigations using comet assay and micronucleus assay. Int J Radiat Biol 2019;95:710-9.
25. Raavi V, Surendran J, Karthik K, et al. Measurement of γ-H2AX foci, miRNA-101, and gene expression as a means to quantify radiation-absorbed dose in cancer patients who had undergone radiotherapy. Radiat Environ Biophys 2019;58:69-80.
26. Guo M, Wang X, Lee F, et al. 0513 Effect of γ radiation on physicochemical properties, protein-protein interaction, and microstructure of whey proteins. Journal of Animal Science 2016; 94:246.
27. Mao A, Liu Y, Zhang H, et al. microRNA expression and biogenesis in cellular response to ionizing radiation. DNA Cell Biol 2014;33:667-79.
28. Anastasov N, Höfig I, Vasconcellos IG, et al. Radiation resistance due to high expression of miR-21 and G2/M checkpoint arrest in breast cancer cells. Radiat Oncol 2012;7:206.
29. Gao F, Liu P, Narayanan J, et al. Changes in miRNA in the lung and whole blood after whole thorax irradiation in rats. Sci Rep 2017;7:44132.
30. Zhang S, Wang W, Gu Q, et al. Protein and miRNA profiling of radiation-induced skin injury in rats: the protective role of peroxiredoxin-6 against ionizing radiation. Free Radic Biol Med 2014;69:96-107.
31. Ghosh SP, Pathak R, Kumar P, et al. Gamma-Tocotrienol Modulates Radiation-Induced MicroRNA Expression in Mouse Spleen. Radiat Res 2016;185:485-95.
32. Powrózek T, Porgador A, Małecka-Massalska T. Detection, prediction, and prognosis: blood circulating microRNA as novel molecular markers of head and neck cancer patients. Expert Rev Mol Diagn 2020;20:31-9.
33. Małachowska B, Tomasik B, Stawiski K, et al. Circulating microRNAs as Biomarkers of Radiation Exposure: A Systematic Review and Meta-Analysis. Int J Radiat Oncol Biol Phys 2020;106:390-402.
34. Wei W, He J, Wang J, et al. Serum microRNAs as Early Indicators for Estimation of Exposure Degree in Response to Ionizing Irradiation. Radiat Res 2017;188:342-54.
35. Jacob NK, Cooley JV, Yee TN, et al. Identification of sensitive serum microRNA biomarkers for radiation biodosimetry. PLoS One 2013;8:e57603.
36. Fendler W, Malachowska B, Meghani K, et al. Evolutionarily conserved serum microRNAs predict radiation-induced fatality in nonhuman primates. Sci Transl Med 2017;9:eaal2408.
37. Cui W, Ma J, Wang Y, et al. Plasma miRNA as biomarkers for assessment of total-body radiation exposure dosimetry. PLoS One 2011;6:e22988.
38. Sun GL, Huang D, Li KR, et al. microRNA-4532 inhibition protects human lens epithelial cells from ultra-violet-induced oxidative injury via activating SIRT6-Nrf2 signaling. Biochem Biophys Res Commun 2019;514:777-84.
39. Oweida AJ, Darragh L, Phan A, et al. STAT3 Modulation of Regulatory T Cells in Response to Radiation Therapy in Head and Neck Cancer. J Natl Cancer Inst 2019;111:1339-49.
40. Zhao C, Du F, Zhao Y, et al. Acute myeloid leukemia cells secrete microRNA-4532-containing exosomes to mediate normal hematopoiesis in hematopoietic stem cells by activating the LDOC1-dependent STAT3 signaling pathway. Stem Cell Res Ther 2019;10:384.
41. Guo S, Lu J, Schlanger R, et al. MicroRNA miR-125a controls hematopoietic stem cell number. Proc Natl Acad Sci U S A 2010;107:14229-34.
42. Zhang Y, Kang R, Liu W, et al. Identification and Analysis of P53-Mediated Competing Endogenous RNA Network in Human Hepatocellular Carcinoma. Int J Biol Sci 2017;13:1213-21.
43. Venkata Narayanan I, Paulsen MT, Bedi K, et al. Transcriptional and post-transcriptional regulation of the

ionizing radiation response by ATM and p53. Sci Rep 2017;7:43598.
44. Zhou B, Luo D. 734 Exosome-mediated miR-4655-3p contributes to UV-radiation induced bystander effects by targeting E2F2. Journal of Investigative Dermatology 2019;139:S127.

(English Language Editor: A. Muijlwijk)

Cite this article as: Li JJ, Xu L, Wang CL, Niu JW, Zou X, Feng XQ, Lu RJ. Changes in patient peripheral blood cell microRNAs after total body irradiation during hematopoietic stem cell transplantation. Ann Transl Med 2022;10(16):857. doi: 10.21037/atm-22-3411

